Nat Hazards (2015) 78:1843–1857
DOI 10.1007/s11069-015-1808-5

ORIGINAL PAPER

An estimation method of soil freeze-thaw erosion in the Qinghai–Tibet Plateau

Bing Guo[1,2] · Yi Zhou[1] · Jinfeng Zhu[1] · Wenliang Liu[1] · Futao Wang[1] · Litao Wang[1] · Lin Jiang[1]

Received: 14 November 2014 / Accepted: 9 May 2015 / Published online: 19 May 2015

Abstract Limited by natural and scientific factors, freeze-thaw (FT) erosion, as a typical erosion process along with wind and water erosion, has not been given enough attention. In this paper, we introduce microwave remote sensing techniques to establish an estimation model of FT erosion. The model includes seven factors: the annual FT cycle days, the average diurnal FT phase-changed water content, average annual precipitation, topographic relief, aspect, annual temperature range and vegetation coverage. The results show that on the whole Qinghai–Tibet Plateau scale, the average intensity of FT erosion belongs to the category of moderate erosion. The spatial extent of the FT erosion region is 163.96 (10^4) km^2, accounting for 63.46 % of the study region. Exhibiting spatial heterogeneity, the distribution of the FT erosion shows an upward trend where the erosion intensity increases from slight erosion in the northwestern region to severe erosion in the southeastern part of the study region. Because of the vast extent of the Qinghai–Tibet

✉ Bing Guo
guobingjl@163.com

Yi Zhou
zhouyi@isas.ac.cn

Jinfeng Zhu
zhf@isas.ac.cn

Wenliang Liu
lwl@isas.ac.cn

Futao Wang
wft@radi.ac.cn

Litao Wang
wlt@radi.ac.cn

Lin Jiang
linlin20061998@126.com

[1] Institute of Remote Sensing and Digital Earth, Chinese Academy of Science, Beijing 100101, China

[2] University of Chinese Academy of Sciences, Shi Jing Shan District, Beijing 100049, China

Plateau, the dominant impact factors for the FT cycle differ over the area. The mid-west plateau is mainly influenced by the annual FT cycle days, average diurnal phase-changed water content and temperature. The southern and southeastern zones are influenced by precipitation, topographic relief and aspect. During the study period, regions which dominated by alpine shrubs were the most severely affected by FT erosion. The results show significance for the understanding of the mechanism and occurrence of FT erosion and therefore provide a scientific basis for the prevention and treatment of FT erosion.

Keywords Freeze-thaw erosion · Microwave remote sensing · Qinghai–Tibet Plateau · Annual FT cycle days · Average diurnal phase-changed water content

1 Introduction

Soil freeze-thaw (FT) erosion is the gravity-induced migration and accumulation process of soil or rocks undergoing mechanical destruction resulting from the expansion and contraction of minerals, induced by volume changes of water at different phases due to the changes in surface soil temperature (Tang 2003; Eigenbrod 1996). During the freezing period, frost heaving occurs when the surface soil moisture migrates to a freezing front under subzero temperatures (Shan et al. 2009; Qi et al. 2008). The mechanical properties of the soil are destroyed by the re-arrangement of the soil particles caused by the frost heave (Niu et al. 2004; Liu et al. 2009). With rising temperature and increased precipitation during the spring melt period, the melting process is significantly exacerbated (Yan et al. 2004; Wang et al. 2001). The melt water, hampered by the unfrozen layers, accumulates during downward infiltration; this significantly increases the water content between the melt layer and the frozen layer. Part or the whole of the shallow slope slides down along the water saturation layer under gravity due to the decreasing stress within the soil particles when the water content reaches saturation or super saturation (Bai et al. 2007; Kok and McCool 1990). In autumn and winter, a portion of the shallow soil water turns into ice as the soil temperature gradually drops below freezing. The adsorbed films, composed of frozen and unfrozen water, become progressively thinner because of the continually falling temperature, which results in more residual liquid water in the pores and crevices of the soil particles (Formanek et al. 1984; Sharratt et al.2002). In addition, a small portion of the soil water may remain in a liquid state at temperatures well below the freezing point of water. Consequently, an upward migration of soil water takes place as frost penetrates the shallow surface soil. Finally, part of or the whole of the shallow slope slides down along the "water saturation layer" under gravity.

During recent decades, global warming has exerted a significant impact on terrestrial ecosystems and these impacts are projected to be even greater in the future (IPCC 2007; Fu et al. 2007).The process of FT erosion has been significantly exacerbated due to the continuously rising temperature and increased precipitation. Unfortunately, in recent decades, this phenomenon is greater than in other regions of the world (Duan et al. 2006; Li and Kang 2006). According to the second national soil erosion data by remote sensing survey, the Qinghai–Tibet Plateau, the main source of the Yangtze, Lancang and Yellow Rivers, suffers severe FT erosion. This disastrous situation has seriously affected production and thereby development of the regional economy (Li et al. 2005). In the Qinghai–Tibet Plateau, the annual freeze-thaw cycle of soils is so significant that it has impacted on

the agricultural and ecological environments (Kang et al. 2010; Liu and Chen 2000). Thus, accurate evaluation of FT erosion on the Qinghai–Tibet Plateau is urgent and necessary for protection of the eco-environment.

A critical limitation to the study of the quantity of FT erosion in the Qinghai–Tibet Plateau is the lack of accurate data, including metrological data, on soil moisture because of its alpine climate and high latitude (Mao et al. 2007; Liu et al. 2009). FT erosion in this region has not attracted enough attention in China and abroad (Bai et al. 2010; Sharratt et al. 2002). Previous studies mainly focused on the soil bulk density, permeability and moisture content (Mostaghimi et al. 1988; Bai et al. 2012; Lee and Lee 2002). The process of soil FT erosion significantly impacts the stability of soil on slopes and their resistance to flowing water (Edwards et al.1995). A thaw-weakened soil is susceptible to water erosion or other exogenic forces (Demidov et al.1995). The resilience modulus is decreased by even a small number of FT cycles (Simonsen and Isacsson 2001). Numerous laboratory studies have been conducted to clarify the impacts of the FT cycles on soil nutrient cycling (Grogan et al. 2004; Reinmann et al. 2012). Caviezel et al. (2014) reveal that shrub encroachment changes soil and vegetation properties, resulting in an increase in resistance to runoff-related erosion processes, but a decrease in slope stability resulting in shallow landslides. Liu et al. (2009) found that the relationships between precipitation, temperature and FT erosion were significant in the FT region of Sichuan Province. The distribution of FT erosion in Tibet was tentatively confirmed by Zhang and Gao (2006). Some studies also suggest that the process of FT erosion greatly affects the physical properties of the soil (Li et al. 2007; Williams and Robinson. 2001).

Assessment of the state of the environment is critical to environmental prediction, management and planning. Thus, we urgently need detailed information on the FT erosion processes in the Qinghai–Tibet Plateau since it is an ecologically vulnerable zone and also an important nature reserve. In this paper, based on the traditional estimation model, we introduce and adopt the indices of microwave remote sensing (annual FT cycle days and average diurnal phase-changed water content) to establish an evaluation model of FT erosion. This is then used to determine the state of the FT erosion and monitor the FT process.

2 Data and methods

2.1 Study area

The Qinghai–Tibet Plateau is located in western China (26°00′12″N–39°46′50″N, 73°18′52″E–104°46′59″E) and has a typical arid and semiarid alpine climate (Chen et al. 2011) (Fig. 1) .It covers an area of 257.24 (10^4) km^2 with the average altitude being about 4000 m above sea level. The temperature ranges from 12 °C in the south to −5 °C in the north, decreasing from higher to lower altitudes (Mao et al. 2007). Precipitation shows great spatial variation from more than 1500 mm in the southeast to 200 mm in the northwest, with 70–80% of total precipitation occurring between May and mid-August. The spatial heterogeneity patterns of precipitation and temperature result in high aridity in most regions with relatively low precipitation and low vegetation coverage. Climate in this region varies from warm-dry in the southeast to warm-wet in the northwest.

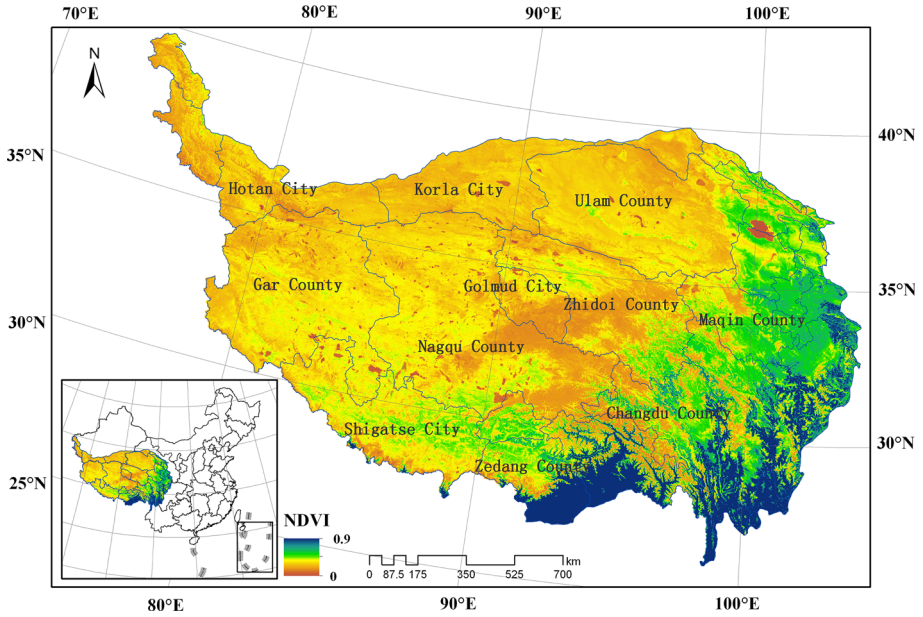

Fig. 1 The location of the Qinghai–Tibet Plateau and the average NDVI in growing season for 2000–2012

2.2 Index variable calculation

It is hard to estimate the quantities of FT erosion for this large-scale region. Currently, few methods are available for measuring the quantities of FT erosion that have been found in China and abroad. Considering the unique impact factors of the FT process in the Qinghai–Tibet Plateau, we chose the seven most critical indices to comprehensively evaluate the quantity of soil FT erosion. These were as follows: the annual FT cycle days, the average diurnal FT phase-changed water content, average annual precipitation, topographic relief, aspect, annual temperature range and average annual vegetation coverage. The spatial resolution of all the datasets (images of the seven indices) was 1 km by 1 km.

2.2.1 Annual FT cycle days

The annual FT cycle day is the number of days that the processes of FT cycles occur in a year. It is a good variable in the FT process and reflects the effects of temperature on the erosion intensity of FT. In this paper, a factor obtained by the images from the microwave remote sensing was introduced to evaluate the intensity of the FT erosion. The Advanced Microwave Scanning Radiometer-EOS (AMSR-E) datasets (available from the National Snow and Ice Data Center, USA) from satellite-borne passive microwave radiometers were used to obtain the land surface brightness temperatures day and night. The changes in the land surface temperature and emissivity were then observed using the inverse of the brightness temperature (Zuerndorfer et al. 1990). In this paper, discriminant analysis algorithms (Eqs. 1, 2) were applied to determine the FT state of the land surface, define the regions experiencing FT cycles and finally calculate the annual FT cycle days (Fig. 2).

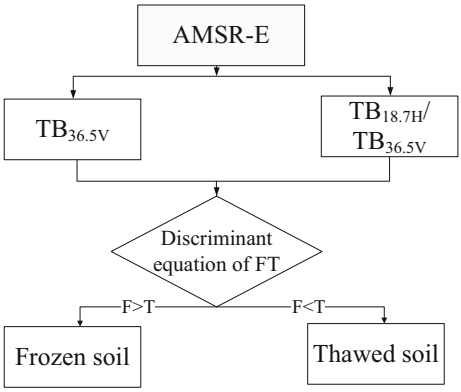

Fig. 2 The calculation process of annual FT cycle days

$$F = 1.47\mathrm{TB}_{36.5\ V} + 91.69\frac{\mathrm{TB}_{18.7\ H}}{\mathrm{TB}_{36.5\ V}} - 226.77 \quad (1)$$

$$T = 1.55\mathrm{TB}_{36.5\ V} + 86.33\frac{\mathrm{TB}_{18.7\ H}}{\mathrm{TB}_{36.5\ V}} - 242.41 \quad (2)$$

where $\mathrm{TB}_{36.5\ \mathrm{V}}$ is the V-polarized brightness temperature of channel 36.5 GHz and $\mathrm{TB}_{18.7\ \mathrm{H}}$ represents the H-polarized brightness temperature of channel 18.7 GHz.

2.2.2 *Average diurnal phase-changed water content*

The phase-changed water content reflects the difference in soil liquid water content during the process of FT cycles (Li et al. 2011; Jackson and Schmugge 1989). The volume expands when liquid water turns into solid ice and this can destroy the structure of soil or rock. The destruction or failure of soil and rock is exacerbated by the increased phase-changed water content. Furthermore, the relationship of microwave emission and soil liquid water content is significant mainly because of the large difference in the dielectric constant between liquid water and dry soil and ice. Thus, soil freeze-thaw processes and the accompanying water phase change can be detected by microwave remote sensing. Therefore, AMSR-E data were used here to estimate the phase-changed water content at the land surface (Fig. 3).

$$M_{\mathrm{pcv}} = A \cdot \left(\frac{\mathrm{TB}_{d,10.65\ H}}{\mathrm{TB}_{d,36.5\ V}} - \frac{\mathrm{TB}_{a,10.65\ H}}{\mathrm{TB}_{a,36.5\ V}}\right) + B \quad (3)$$

where M_{pcv} refers to the phase-changed water content, subscript d indicates the descending orbit and subscript a indicates the ascending orbit. A and B are regression coefficients.

2.2.3 *Annual average precipitation*

Precipitation is a main contributor to soil erosion especially in arid and semiarid regions (Okin et al. 2001).The water content of soil is influenced by precipitation and shows a significant relationship with the intensity of FT erosion. Also, precipitation and melt water are the important driving forces in the movement of FT erosion materials. The meteorological data used here were obtained from the Climatic Information Center of Tibet Autonomous Region, China (http://cdc.cma.gov.cn/home.do). However, the distribution of meteorological stations was uneven. Therefore, interpolated stations were constructed

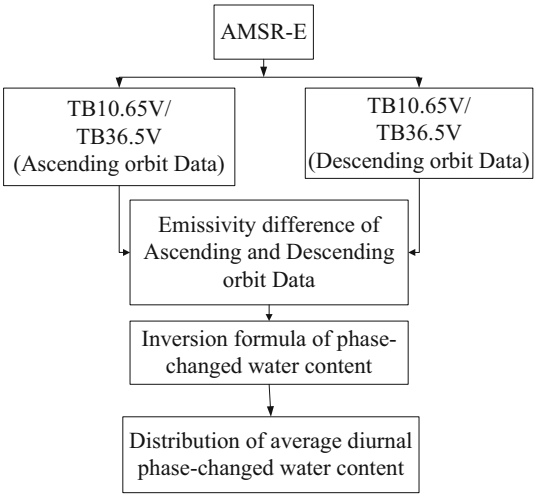

Fig. 3 The calculation process of average diurnal phase-changed water content

using the Tropical Rainfall Measuring Mission(TRMM)with Eq. 4 (Jia et al. 2011). This equation was used to calibrate the TRMM 3B42 precipitation.

$$T_R = 2.048 \cdot V^{0.823} \tag{4}$$

where V (mm year^{-1}) represents TRMM3B42-derived annual precipitation and T_R (mm year^{-1}) is the annual rainfall observed by the meteorological stations during 2000–2012.

2.2.4 Aspect

Aspect can greatly influence the amount of solar radiation received on the ground. There is a large amount of solar radiation incident on sunny slopes leading to large soil temperature differences between day and night; this significantly exacerbates the intensity of FT erosion. However, the change of solar radiation on a shady slope is small so the soil temperature difference between day and night is not noticeable. Therefore, the intensity of FT erosion in these zones is small. Aspect here is calculated using the Spatial Analyst Tools of ArcGIS 10.1 based on a 90-m digital elevation model (DEM) (http://datamirror.csdb.cn), obtained from the National Geospatial-Intelligence Agency (NGA) and the National Aeronautics and Space Administration (NASA).

2.2.5 Topographic relief

Topographic relief can be defined as the difference in altitude between the highest and lowest point within certain region. It can affect the velocity and transport distance of the FT erosion materials and can contribute significantly to FT erosion.

$$\mathrm{TR} = H_{\max} - H_{\min} \tag{5}$$

where TR represents the value of topographic relief within an $n \times n$ average sliding window, $H_{\max}$ is the maximum value of the sliding window, and $H_{\min}$ is the minimum value of the sliding window. Topographic relief is here calculated via Eq. 5 based on a 90-m digital elevation model (DEM).

2.2.6 Vegetation coverage

Vegetation (canopy, understory and plant roots) is of great importance for regulating surface hydrological processes (Zhang and Gao 2006; Chen et al. 2007). The above-ground parts of the plants can mitigate the erosion forces of rainfall, while the below-ground parts increase the soil stability and reduce destructive effects on soil (Chen et al. 2007). In addition, vegetation can reduce the soil temperature difference between day and night, so it plays an important role in the FT erosion process.

The Normalized Difference Vegetation Index (NDVI, Huete and Tucker 1991) is a measure of vegetation activity and biomass. In this paper, the Spot-Vegetation NDVI data with 1 km by 1-km resolution for every 10 days from April 2000 to December 2012 were adopted. The 10-day periods were defined as the 1st to the 10th, 11th to the 20th and 21st to the end of each month. The monthly NDVI was obtained by the maximum value composite method, which minimizes cloud contamination, atmospheric effects and solar zenith angle effects (Hope et al. 2003; Stow et al. 2004). Thus, the average annual vegetation coverage was obtained based on the monthly NDVIs. Here, the following equation was employed to invert the vegetation fraction:

$$\mathrm{FVC} = \left(\frac{\mathrm{NDVI} - \mathrm{NDVIsoil}}{\mathrm{NDVIveg} - \mathrm{NDVIsoil}}\right)^{L} \tag{6}$$

where FVC is the fractional vegetation coverage, NDVIveg is the maximum value of pure vegetation at a confidential level (CL) of 0.95, NDVIsoil refers to the minimum value of pure bare soil (CL = 0.95), and L is an experience factor, its value is 1.1 in this paper.

2.2.7 Annual temperature range

Soil temperature is a crucial factor influencing the FT erosion process, and it determines the frozen-thawed depth of the surface soil layer (Li et al. 2005). The larger the soil temperature range, the more severe the FT erosion. Moreover, the change range and intensity of the soil temperature around 0 °C exhibit a negative relationship with the stability of physical properties and the erosion resistance of soil (Lee and Lee 2002). The larger the change in soil temperature, the more severe the FT erosion. However, soil temperatures could not be obtained on a large scale in the Qinghai–Tibet Plateau due to the lack of long-term observations. In this study, we used the data from 126 meteorological stations around the study region and found that the annual temperature range, latitude, longitude and attitude showed significant multiple linear relationships.

$$T_{\mathrm{atr}} = 3.2103 + 1.2571X_1 - 0.2099X_2 - 0.0003887X_3 \tag{7}$$

where the T_{atr} is the annual temperature range, X_1 represents latitude, X_2 is longitude, and X_3 refers to the altitude. These three factors were obtained based on the DEM.

2.3 Evaluation model of FT erosion

The evaluation of FT erosion requires the integration of multiple factors to obtain a comprehensive evaluation index. However, most previous studies used only the analytic hierarchy process (AHP) or an entropy method to calculate the weight of each index. The results of the AHP are mostly influenced by subjectivity, while those of the entropy method often ignore the experience and knowledge of experts (Pinzon et al. 2005). In this paper,

Table 1 Classification assignments of evaluation indices and their weights of AHP, entropy method, and the improved AHP

Index	Assignment criteria					Weight		
						AHP_i	EM_i	$AHP–EM_i$
Annual FT cycle days (day)	≤50	50–100	100–150	150–200	>200	0.16	0.18	0.2
Aspect(°)	0–36 324–360	36–72 288–324	72–108 252–288	108–144 216–252	144–216	0.06	0.12	0.05
Average diurnal phase–changed water content (%)	≤0.05	0.05–0.08	0.08–0.11	0.11–0.14	>0.14	0.15	0.17	0.18
Annual temperature range (°C)	≤18	18–20	20–22	22–24	>24	0.19	0.1	0.13
Topographic relief (m)	≤50	50–100	100–300	300–500	>500	0.24	0.13	0.22
Average annual precipitation (mm)	≤100	100–250	250–400	400–550	>550	0.06	0.14	0.06
Vegetation coverage (%)	>75	75–60	60–45	45–30	≤30	0.14	0.16	0.16
Assigned value	1	3	5	7	9			

we combined the two methods to obtain a weighting of indices so that the experience and knowledge of experts and the objective information quantity of each index could be considered. Then, we adapted the improved AHP and applied a weighted summation method to obtain the comprehensive evaluation index using the following equations:

$$W_{\mathrm{AHP-EM},i} = \frac{\mathrm{EM}_i \mathrm{AHP}_i}{\sum_{i=1}^{n} \mathrm{EM}_i \mathrm{AHP}_i} \tag{8}$$

$$I = \frac{\sum_{i=1}^{n} W_{\mathrm{AHP-EM},i} I_i}{\sum_{i=1}^{n} W_{\mathrm{AHP-EM},i}} \tag{9}$$

where $W_{\mathrm{AHP\text{-}EM,i}}$ is the modified weight of each index, EM_i is the weight obtained by entropy method, AHP_i is the weight obtained by AHP, I_i is the dimensionless value of each index, n refers to the number of impact factors, and I is the comprehensive evaluation index.

Firstly, the EM_i was obtained by the entropy method; then, it was taken into the calculation of $\mathrm{W}_{\mathrm{AHP\text{-}EM},\ i}$ with AHP_i. The values of the weightings are listed in Table 1, and some typical classification factors are shown in Fig. 4.

3 Results

3.1 Classification map of FT erosion and accuracy assessment

Based on Eqs. (8, 9) and Table 1, the evaluation of FT erosion was obtained using seven indices: the annual FT cycle days, the average diurnal phase-changed water content, average annual precipitation, average vegetation coverage, topographic relief, aspect and the annual temperature range.

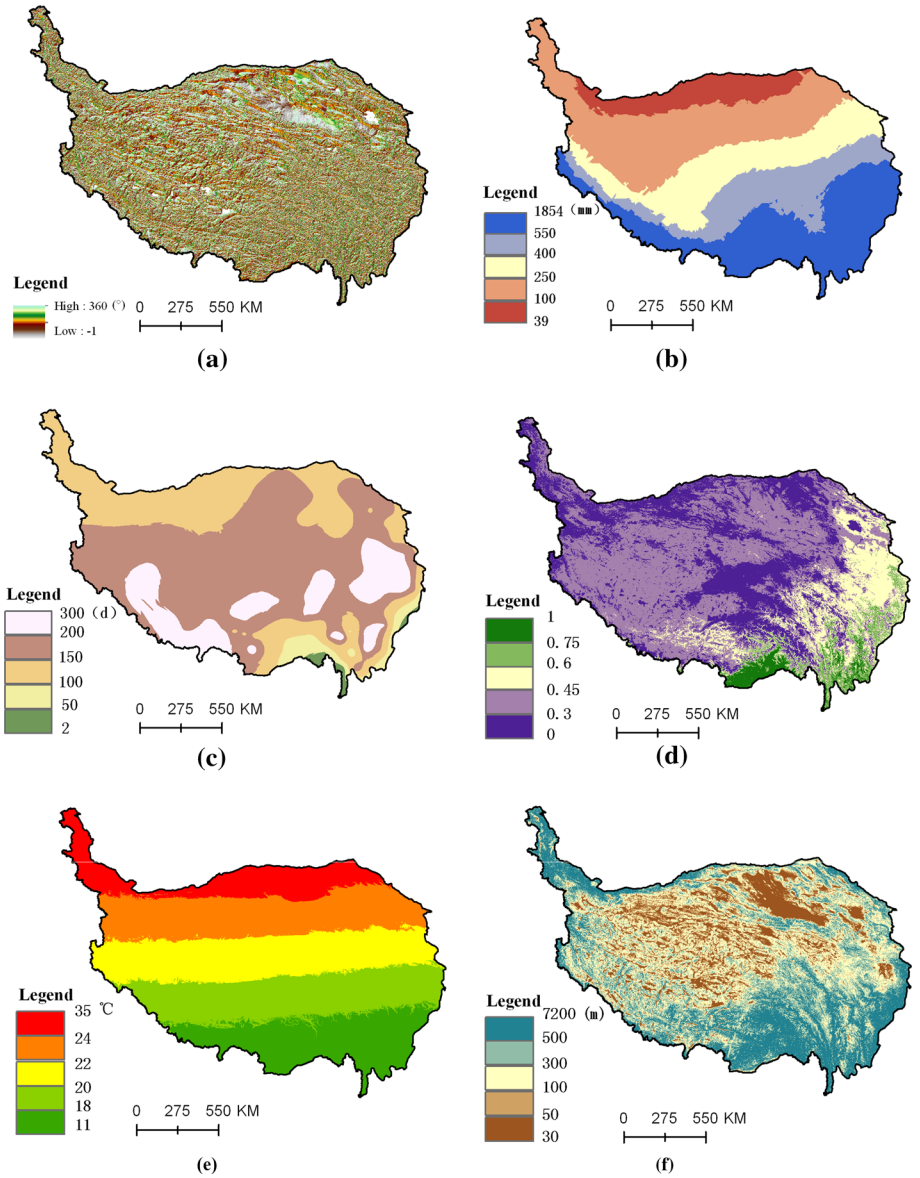

Fig. 4 Distribution maps of typically classified indices. **a** Aspect; **b** annual precipitation annual FT cycle days; **c** annual precipitation; **d** vegetation coverage; **e** annual temperature range; **f** topographic relief

The FT erosion was then divided into six categories: No-FT erosion ($I < 3.4$), slight erosion ($3.4 < I < 4.9$), mild erosion ($4.9 < I < 5.5$), moderate erosion ($5.5 < I < 6.2$), intensive erosion ($6.2 < I < 7.0$) and severe erosion ($7.0 < I < 8.4$). The spatial patterns of the FT erosion are shown in Fig. 5.

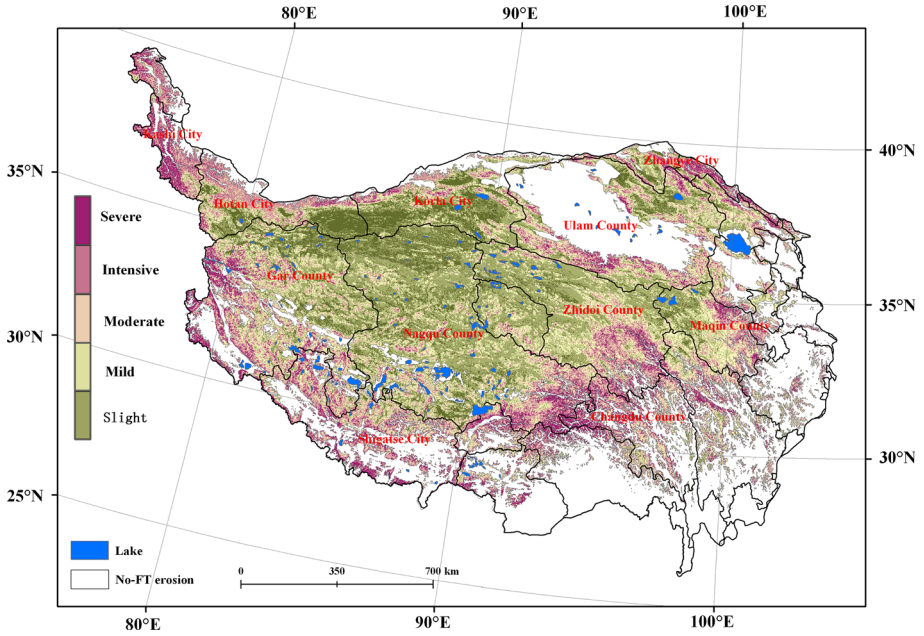

Fig. 5 Classification map of the quantity of freeze-thaw erosion in the Qinghai–Tibet Plateau

Table 2 Error matrix of FT erosion categories

Levels of sampling points	Evaluated value of FT erosion					
	Slight erosion	Mild erosion	Moderate erosion	Intensive erosion	Severe erosion	Sum
Slight erosion	135	4	3	1	2	145
Mild erosion	2	21	3	3	2	31
Moderate erosion	3	5	39	3	1	51
Intensive erosion	1	1	2	15	2	21
Severe erosion	1	1	0	1	17	20
Sum	142	32	47	23	24	268

A basic error matrix and precision index were applied to test the accuracy of the results. In order to confirm the validity of the sampling points, we chose a total of 268 sites (Table 2) from regions with different landforms, aspect, plant types, land-use types and so on. The error matrix of the calculated erosion category and the field survey is shown in Table 3.

As shown in Table 3, the cartographic precision of all categories ranged from 0.68 to 0.93, which demonstrates the validity of the classification. Slight erosion showed the best precision, while the accuracies of mild and intensive erosion were much lower. However, the overall precision was 84.7 %, confirming the high efficiency and accuracy of this freeze-thaw erosion model for the Qinghai–Tibet Plateau.

Table 3 Precision index of FT erosion categories

Precision Test	User accuracy	Commission	Cartographic accuracy	Omission
Slight erosion	0.95	0.05	0.93	0.07
Mild erosion	0.66	0.34	0.68	0.32
Moderate erosion	0.83	0.17	0.76	0.24
Intensive erosion	0.65	0.35	0.71	0.29
Severe erosion	0.71	0.29	0.85	0.15

Table 4 Area and area ratios of different categories of FT erosion intensity

	Slight erosion	Mild erosion	Moderate erosion	Intensive erosion	Severe erosion
Area ((10^4) km^2)	22.79	48.25	45.72	31.87	15.28
Percentage (%)	13.90	29.44	27.89	19.44	9.32

3.2 Spatial differentiation of FT erosion

Figure 5 shows that FT erosion is widely distributed in the Qinghai–Tibet Plateau .It covers about 63.46 %, an area of 163.96 (10^4) km^2 . FT erosion was discontinuously distributed in the mid-western region (30°–40°N, 80°–100°E). The No-FT region was mainly concentrated in the southern and southeastern regions and in Ulam County. The average intensity of FT erosion for the whole region was 5.77, placing it in the category of moderate erosion. Among the grades of FT erosion, mild erosion covered the largest region with an area of 48.25 (10^4) km^2, accounting for 29.44 % of the erosion area. In addition, the zones of slight, moderate, intensive and severe erosion were 22.79 (10^4), 45.72 (10^4), 31.87 (10^4) and 15.28 (10^4) km^2 with percentages of 13.90, 27.89, 19.44 and 9.32 % of the total erosion area, respectively (Table 4).

The spatial disparities of different FT erosion zones differed significantly.

The zone of slight erosion was mainly concentrated in northern part of the region, in southern Hortan City, mid-southern Korla City and northern Nagqu County. Of all the FT erosion zones, the mild erosion zone was the most widely distributed and covered almost the whole erosion region of the Qinghai–Tibet Plateau. The zone of moderate erosion was discontinuously distributed in the southern and northern mountain regions, occupying the western Car County, northern Hotan City and southern Maqin County. Similar to the moderate erosion, the intensive erosion zone was also widely distributed and included Shigatse City, northern Changdu County and western Gar County. The zone of severe erosion was mainly concentrated in the southern mountains and the plateau of western Sichuan.

4 Discussion

4.1 Improvement of the model for FT erosion

The Qinghai–Tibet Plateau, the highest and largest plateau on the earth, is the major region of FT erosion in China. However, enough attention has not been paid to this issue either in China or abroad. Compared with wind and water erosion, the studies on FT erosion are few.

The traditional models of FT erosion are not very accurate and largely inadequate because of the lack of reliable data on factors such as temperature, land use, soil types, vegetation cover and annual precipitation (Kok and McCool 1990; Zhang et al. 2007). In this paper, microwave remote sensing techniques were introduced to determine the state of and detect the processes of FT erosion. Based on the images from microwave remote sensing (AMSR-E), we monitored the soil sensitivity due to the changes in moisture and calculated the annual FT cycle days and average diurnal phase-changed water content. These indices better reflect the whole process of the FT cycle (Li et al. 2005). The results of the accuracy assessment indicated that the improved model of FT erosion was efficient and was applicable to the Qinghai–Tibet Plateau.

4.2 The relationship between FT erosion, climate and terrain

Our results suggested that the spatial distribution of FT erosion intensity increased from slight erosion in the northwest of the region to severe erosion in southern part, but the determining factors were different. The slight erosion zone was mainly concentrated in the northern region, northern Gar County and northern Nagqu County, as here precipitation is scarce and the slopes much smaller. The zone of mild erosion was distributed between slight and moderate erosion. In the middle of the Qinghai–Tibet Plateau, the topographic relief and slope are much smaller and the dominant impact factors are temperature, annual FT cycle days and aspect. In the southern foot of the Himalayas and downstream of the Brahmaputra basin, warm, moist air from the Indian Ocean often brings abundant rainfall (Yu et al. 2003). In addition, high mountains are widely distributed in the southern and southeastern regions (30°–34°N, 93°–100°E), which results in larger slope and topographic relief. Thus, intensive erosion and severe erosion were concentrated in these regions. Most of Ulam County belongs to the No-FT erosion category due to the low altitude and flat terrain. In addition in the southern Qinghai–Tibet Plateau regions (28°–30°N, 87°–105°E and 30°–38°N, 101°–105°E), the process of FT erosion does not exist because of the high temperatures and vegetation cover.

The plateau has experienced significant warming during the past decades (Liu and Chen 2000), and this warming is predicted to continue in the twenty-first century (IPCC 2007). In addition, the environmental fragility created by the unique geographical conditions of the Qinghai–Tibet Plateau tends to be sensitive to climate change (Niu et al. 2004). Increasing rainfall and rising temperatures will increase the intensity of FT erosion, especially in the mid-western region with its sparse vegetation cover and large annual FT cycle days. In addition, the eco-environment has been significantly affected by human activities, including deforestation, overgrazing and construction (Zhang et al. 2007). These activities decrease the vegetation coverage and destroy the physical and chemical structure of the soil. Both natural and anthropogenic factors aggravate the process of FT erosion. Thus, it is urgent for us to pay more attention to the prevention and treatment of FT erosion.

4.3 Relationship between FT erosion and plant types

To explore the relationship between plants and FT erosion, six typical types of plant (subalpine coniferous forest (SCF), broadleaf forest (BF), alpine shrubs (AS), meadow (MD), sparse cushion vegetation (SCV) and desert (DS)) were chosen to examine how plants influence the process of FT erosion (Fig. 6). The region dominated by AS showed the largest intensity of FT erosion with an average of 6.96, i.e., severe erosion. This phenomenon resulted from the fact that the AS is mainly distributed in the mountains of the

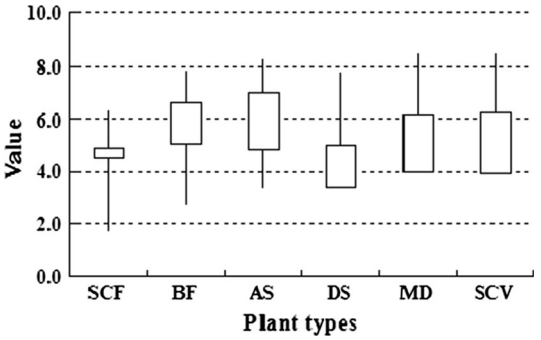

Fig. 6 Change intensity of FT erosion for each plant type. The *top* of box represents mean value of FT erosion intensity for each plant type; the bottom of box refers to minimum value; the *top* of line represents the maximum value; the bottom of line refers to the fluctuation range of FT erosion intensity. SCF, subalpine coniferous forest; BF, broadleaf forest; AS, alpine shrubs; DS, desert; MD, meadow; SCV, sparse cushion vegetation

southeastern region that exhibit larger topographic relief and precipitation. The mean intensities of FT erosion for BF and SCV were 6.57, 6.23, respectively, i.e., intensive erosion. The fluctuation range of SVC was the largest due to its wide distribution and low vegetation fraction, followed by MD. The SCF had the smallest fluctuation range of FT erosion intensity because the plant types were concentrated in the mid-low mountains of the southeastern region where the erosion intensity was mainly intensive. The desert represented a zone with no or sparse vegetation, and it was mainly distributed in the northwestern plateau where precipitation was scare and the landforms much lower. Thus, the mean intensity in this zone belonged to mild erosion. By comparing the mean and fluctuation range of FT erosion intensity for each plant type, it was found that during the study period, regions which dominated by alpine shrubs were the most severely affected by FT erosion, followed by SCF and SCV. In addition, zones with sparse cushion vegetation were potentially the worst-hit area by FT erosion, exhibiting the largest fluctuation range.

5 Conclusions

In this study, we introduced the microwave remote sensing technique to establish an estimation model of FT erosion. The estimated results were proved to be accurate by precision testing with the field sampling data.

The region of FT erosion was widely distributed in the Qinghai–Tibet Plateau, covering 163.96 (10^4) km^2 and accounting for 63.46 % of the area. The average intensity of FT erosion over the whole region was moderate erosion category. The erosion intensity increased from slight erosion in northwestern regions to severe erosion in the southeastern part. Due to the great environmental heterogeneity, the dominant impacting factors for the FT cycle were different across the region. The mid-western plateau was mainly influenced by the annual FT cycle days, average diurnal phase-changed water content and temperature. The southern and southeastern zones were influenced by precipitation, topographic relief and aspect. However, further studies need to be conducted to clarify the mechanisms underlying the process of FT erosion and strengthen the precision of the evaluation process.

Acknowledgments This work was supported by Foundation of Director of Institute of Remote Sensing and Digital Earth, Chinese Academy of Science (Y4SY0200CX) and Special Project on High Resolution of Earth Observation System for Major Function Oriented Zones Planning (No. 00-Y30B14-9001-14/16).

References

Bai JH, Deng W, Wang Q et al (2007) Spatial distribution of inorganic nitrogen contents of marsh soils in a river floodplain with different flood frequencies from soil-defrozen period. Environ Monit Assess 134(3):421–428. doi:10.1007/s10661-007-9633-2

Bai JH, Ouyang H, Xiao R et al (2010) Spatial variability of soil carbon, nitrogen, and phosphorus content and storage in an alpine wetland in the Qinghai–Tibet Plateau, China. Aust J Soil Res 48(8):730–736. doi:10.1071/SR09171

Bai JH, Gao HF, Xiao R et al (2012) A review of soil nitrogen mineralization as affected by water and salt in coastal wetlands: issues and methods. Clean Soil Air Water 40(10):1099–1105. doi:10.1002/clen.201200055

Caviezel C, Hunziker M, Schaffner M et al (2014) Soil-vegetation interaction on slopes with bush encroachment in the central Alps—adapting slope stability measurements to shifting process domains. Earth Surface Process Landforms 39(4):509–521. doi:10.1002/esp.3513

Chen SQ, Wen LJ, Lv SH et al (2007) Study of NDVI and climate change in Maqu County, upstream of Yellow river. J Glaciol Geocryol 29(1):131–136 **(In Chinese)**

Chen H, Zhu Q, Wu N et al (2011) Delayed spring phenology on the Tibetan Plateau may also be attributable to other factors than winter and spring warming. Proc Natl Acad Sci USA 108(19):93–99. doi:10.1073/pnas.1100091108

Demidov VV, Ostroumov VY, Nikitishena IA et al (1995) Seasonal freezing and soil erosion during snowmelt. Eurasian Soil Sci 28(10):78–87

Duan AM, Wu GX, Zhang Q (2006) New proofs of the recent climate warming over the Tibetan Plateau as a result of the increasing greenhouse gases emissions. Chin Sci Bull 51(11):1396–1400. doi:10.1007/s11434-006-1396-6

Edwards LM, Burney JR, Frame PA (1995) Rill sediment transport on a Prince Edward Island (Canada) fine sandy loam. Soil Technol 8(2):127–138. doi:10.1016/0933-3630(95)00009-2

Eigenbrod KD (1996) Effects of cyclic freezing and thawing on volume changes and permeabilities of soft fine grained soils. Can Geotech J 33(4):529–537

Formanek GE, McCool DK, Papendick RI (1984) Freeze thaw and consolidation effects on strength of a wet silt loam. Trans Am Soc Agric Eng 27(6):1749–1752

Fu XF, Yang ST, Liu CM (2007) Changes of NDVI and their relations with principal climatic factors in the Yarlung Zangbo River Basin. Geogr Res 26(1):60–66 **(In Chinese)**

Grogan P, Michelsen A, Ambus P et al (2004) Freeze-thaw regime effects on carbon and nitrogen dynamics in sub-arctic heath tundra mesocosms. Soil Biol Biochem 36(4):641–654. doi:10.1016/j.soilbio.2003.12.007

Hope A, Boynton W, Stow D (2003) Interannual growth dynamics of vegetation in the Kuparuk River watershed based on the normalized difference vegetation index. Int J Remote Sens 24(17):3413–3425. doi:10.1080/0143116021000021170

Huete AR, Tucker CJ (1991) Investigation of soil influences in AVHRR red and near-infrared vegetation index imagery. Int J Remote Sens 12(6):1223–1242

IPCC (2007) Climate change 2007: the physical science basis. Contribution of working group I. In: Solomon S, Qin D, Manning M, Chen Z, Marquis M, Averyt KB, Tignor M, Miller HL (eds) Fourth assessment report of the intergovernmental panel on climate change, Cambridge University Press, Cambridge, UK

Jackson TJ, Schmugge TJ (1989) Passive microwave remote-sensing system for soil-moisture- some supporting research. IEEE Trans Geosci Remote Sens 27(2):225–235. doi:10.1109/36.20301

Jia SF, Zhu WB, Lu AF et al (2011) A statistical spatial downscaling algorithm of TRMM precipitation based on NDVI and DEM in the Qaidam Basin of China. Remote Sens Environ 115(12):3069–3079. doi:10.1016/j.rse.2011.06.009

Kang SC, Xu YW, You QL et al (2010) Review of climate and cryospheric change in the Tibetan Plateau. Environ Res Lett 5(1):15–23. doi:10.1088/1748-9326/5/1/015101

Kok H, McCool DK (1990) Quantifying freeze/thaw–induced variability of soil strength. Trans Am Soc Agric Eng 33(2):501–506

Lee J, Lee S (2002) The frost penetration with the modified soil in the landfill bottom liner system. Geosci J 6(1):7–12

Li CL, Kang SC (2006) Review of studies in climate change over the Tibetan Plateau. Acta Geogr Sin 61(3):327–335 **(In Chinese)**

Li HX, Liu SZ, Zhong XH et al (2005) GIS–based sensitivity evaluation on freeze–thaw erosion in Tibet. Soil Water Conserv China 7(2):44–46 **(In Chinese)**

Li RP, Shi HB, Takeo A et al (2007) Characteristics of air temperature and water–salt transfer during freezing and thawing period. Trans Chin Soc Agric Eng 23(4):70–74 **(In Chinese)**

Li SH, Zhou DM, Luan ZQ et al (2011) Quantitative simulation on soil moisture contents of two typical vegetation communities in Sanjiang Plain, China. Chin Geogr Sci 21(6):723–733. doi:10.1007/s11769-011-0507-8

Liu XD, Chen BD (2000) Climatic warming in the Tibetan Plateau during recent decades. Int J Climatol 20(14):1729–1742. doi:10.1002/1097-0088(20001130)20:14<1729:AID-JOC556>3.0.CO;2-Y

Liu XD, Cheng ZG, Yan LB (2009) Elevation dependency of recent and future minimum surface air temperature trends in the Tibetan Plateau and its surroundings. Global Planet Change 68(3):164–174. doi:10.1016/j.gloplacha.2009.03.017

Mao F, Lu ZG, Zhang JH et al (2007) Relations between AVHRR NDVI and climate factors in Northern Tibet in recent 20 years. Acta Ecologica Sin 27(8):3198–3205 **(In Chinese)**

Mostaghimi S, Young RA, Wilts AR et al (1988) Effects of frost action on soil aggregate stability. Trans Am Soc Agric Eng 31(2):435–439

Niu FS, Cheng GD, Lai YM et al (2004) Instability study on thaw slumping in permafrost regions of Qinghai–Tibet Plateau. Chin J Geotech Eng 26(3):402–406 **(In Chinese)**

Okin GS, Murray B, Schlesinger WH (2001) Degradation of sandy arid shrubland environments: observations, process modelling, and management implications. J Arid Environ 47(2):123–144. doi:10.1006/jare.2000.0711

Pinzon J, Brown ME, Tucker CJ (2005) Satellite time series correction of orbital drift artifacts using empirical mode decomposition. In: Huang NE, Shen SSP (eds) EMD and its applications, vol 10. World Scientific, Singapore, pp 285–295

Qi J, Ma W, Song C (2008) Influence of freeze–thaw on engineering properties of a silty soil. Cold Reg Sci Technol 53(3):397–404. doi:10.1016/j.coldregions.05.010

Reinmann AB, Templer PH, Campbell JL (2012) Severe soil frost reduces losses of carbon and nitrogen from the forest floor during simulated snowmelt: a laboratory Experiment. Soil Biol Biochem 44(1):65–74. doi:10.1016/j.soilbio.2011.08.018

Shan W, Guo Y, Liu H (2009) Effect of freeze–thaw on strength and microstructure of salty clay. J Harbin Inst Technol 16(1):207–211 **(In Chinese)**

Sharratt BS, Lindstrom MJ, Benoit GR et al (2002) Runoff and soil erosion during spring thaw in the northern U.S Corn Belt. J Soil Water Conserv 55(4):487–494

Simonsen E, Isacsson U (2001) Soil behavior during freezing and thawing using variable and constant confining pressure triaxial tests. Can Geotech J 38(4):863–875

Stow D, Hope A, McGuire D et al (2004) Remote sensing of vegetation and land–cover change in Arctic Tundra Ecosystems. Remote Sens Environ 89(3):281–308. doi:10.1016/j.rse.2003.10.018

Tang KL (2003) Soil and water conservation in China. Science Press, Beijing, pp 3–27

Wang G, Qian J, Cheng G (2001) Eco-environmental degradation and causal analysis in the source region of the Yellow River. Environ Geol 40(7):884–890 **(In Chinese)**

Williams RBG, Robinson DA (2001) Experimental frost weathering of sandstone by various combinations of salts. Earth Surf Proc Land 26(8):811–818. doi:10.1002/esp.227

Yan P, Dong GR, Su ZZ et al (2004) Desertification problems in the Yangtze River source area, China. Land Degrad Dev 15(2):177–182. doi:10.1002/ldr.602

Yu FF, Price KP, Ellis J et al (2003) Response of seasonal vegetation development to climatic variations in eastern central Asia. Remote Sens Environ 87(1):42–54. doi:10.1016/S0034-4257(03)00144-5

Zhang WJ, Gao ZQ (2006) Spatial variation of water/thermal elements and NDVI with altitudes in central and eastern Tibetan Plateau. Geogr Res 25(5):877–886 **(In Chinese)**

Zhang JG, Liu SZ, Yang SQ (2007) The classification and assessment of freeze–thaw erosion in Tibet. J Geog Sci 17(2):165–174. doi:10.1007/s11442-007-0165-z

Zuerndorfer BW, England AW, Dobson MC et al (1990) Mapping freeze/thaw boundaries with SMMR data. Agric For Meteorol 52(1–2):199–225. doi:10.1016/0168-1923(90)90106-G